Fatty acid amide hydrolase shapes NKT cell responses by influencing the serum transport of lipid antigen in mice

Stefan Freigang,[1] Victoria Zadorozhny,[1] Michele K. McKinney,[2] Philippe Krebs,[1] Rana Herro,[1] Joanna Pawlak,[1] Lisa Kain,[1] Nicolas Schrantz,[1] Kim Masuda,[2] Yang Liu,[3] Paul B. Savage,[3] Albert Bendelac,[4,5] Benjamin F. Cravatt,[2] and Luc Teyton[1]

[1]Department of Immunology and [2]Department of Chemical Physiology, The Scripps Research Institute, La Jolla, California, USA. [3]Department of Chemistry, Brigham Young University, Provo, Utah, USA. [4]Committee on Immunology, University of Chicago, Chicago, Illinois, USA. [5]Howard Hughes Medical Institute, Chevy Chase, Maryland, USA.

The potent regulatory properties of NKT cells render this subset of lipid-specific T cells a promising target for immunotherapeutic interventions. The marine sponge glycolipid α-galactosylceramide (αGalCer) is the prototypic NKT cell agonist, which elicits this function when bound to CD1d. However, our understanding of the in vivo properties of NKT cell agonists and the host factors that control their bioactivity remains very limited. In this report, we isolated the enzyme fatty acid amide hydrolase (FAAH) from mouse serum as an αGalCer-binding protein that modulates the induction of key effector functions of NKT cells in vivo. FAAH bound αGalCer in vivo and in vitro and was required for the efficient targeting of lipid antigens for CD1d presentation. Immunization of *Faah*-deficient mice with αGalCer resulted in a reduced systemic cytokine production, but enhanced expansion of splenic NKT cells. This distinct NKT response conferred a drastically increased adjuvant effect and strongly promoted protective CTL responses. Thus, our findings identify not only the presence of FAAH in normal mouse serum, but also its critical role in the tuning of immune responses to lipid antigens by orchestrating their transport and targeting for NKT cell activation. Our results suggest that the serum transport of lipid antigens directly shapes the quality of NKT cell responses, which could potentially be modulated in support of novel vaccination strategies.

Introduction

The NKT cell population represents a specialized subset of lipid antigen-specific T cells with important regulatory functions (1–3). NKT cells are characterized by the expression of an invariant Vα14-Jα18/Vβ8 (Vα24-Jα18/Vβ11 in humans) TCR in combination with NK cell markers, e.g., CD161 (NK1.1). Via their TCRs, NKT cells recognize endogenous (4) and microbial (5–8) glycolipid antigens presented by the major histocompatibility class I–like molecule CD1d. NKT cells have been implicated in a variety of antimicrobial, antitumoral, and autoimmune responses (2, 3). Upon activation, NKT cells rapidly release large quantities of cytokines, mainly IFN-γ and IL-4, and induce DC maturation in a NKT/DC feedback loop that involves IL-12, CD40/CD40 ligand interactions, and subsequent IFN-γ release from NK cells (9, 10). Thus, NKT cells directly influence the early stages of immune activation and modulate the priming of the adaptive immune response. NKT cell agonists, such as the prototypic NKT cell antigen αGalCer, therefore offer a great potential as novel vaccine adjuvants. Indeed, experimental NKT cell activation markedly enhances the ability of protein vaccines to induce specific T and B cell responses (11–13). Furthermore, NKT cells have been shown to contribute to immunity against tumors in murine models (14, 15), and the efficacy of αGalCer is currently being evaluated in cancer patients in phase I trials (16–19). However, the first clinical trials as well as recent research findings suggest that a much better understanding of the pharmacology of lipid antigens is required in order to improve clinical outcomes.

In particular, it has become more and more evident that distinct subsets of NKT cells exist in vivo that exhibit substantially distinct effector functions (20–24). As a consequence, current vaccination protocols need to be refined in order to expand the appropriate NKT cell subset and to induce a beneficial cytokine profile. One factor that very likely contributes to the initial tissue distribution and dynamics of CD1d antigen presentation at immunological sites is the association and transport of lipid antigens with serum components. For example, by mediating cellular uptake via the LDL receptor (LDLR), the VLDL fraction and its apoE essentially control the CD1d presentation of digalactosylceramides (25). However, apart from this apolipoprotein-mediated uptake pathway, little is known about host factors that control NKT cell expansion and modulate the targeting of lipid antigens for CD1d presentation in vivo.

FAAH is the primary enzyme degrading fatty acid amides, a class of endogenous lipid signaling molecules (26, 27). FAAH belongs to the large family of amidase signature enzymes, most of which are of bacterial and fungal origin. Unlike many of its soluble microbial relatives, FAAH is an integral membrane protein located on the cytosolic leaflet of the endoplasmic reticulum membrane (28, 29). The most prominent substrates of FAAH are endocannabinoids, fatty acid amides that activate cannabinoid (CB) receptors. Through hydrolysis of endocannabinoids, FAAH terminates CB receptor signaling and controls the endocannabinoid tone. Accordingly, *Faah*-deficient animals have elevated endocannabinoid levels in their tissues, show characteristics of CB receptor activation, and are supersensitive to exogenous CBs (30). In addition, *Faah*-deficient

Conflict of interest: The authors have declared that no conflict of interest exists.
Citation for this article: *J Clin Invest.* 2010;120(6):1873–1884. doi:10.1172/JCI40451.

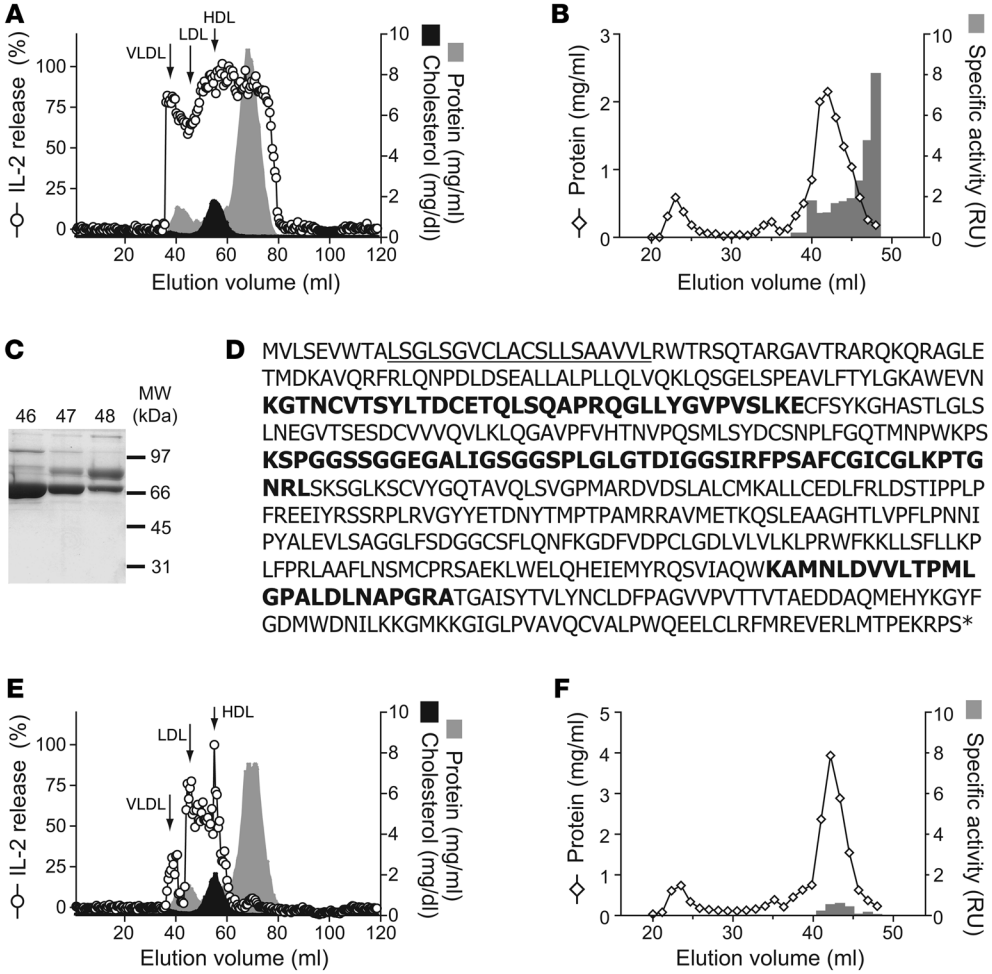

Figure 1
Identification of fatty acid amide hydrolase as an αGalCer-binding protein in serum. (**A**) Distribution of αGalCer in serum of WT mice (white circles) after fractionation by gel filtration chromatography as detected by DN32.D3 NKT hybridoma cells in an antigen presentation assay. Distribution of lipoproteins and proteins was determined by the cholesterol (black histogram) and protein (gray histogram) concentration of individual fractions. (**B**) Fractionation of serum proteins from WT mice (pooled fractions eluting 65–80 ml in **A**) by anion exchange chromatography. The protein concentration (white diamonds) and specific stimulatory activity (gray bars) of individual fractions are shown. (**C**) SDS-PAGE analysis of fractions from **B**. (**D**) Amino acid sequence of murine FAAH. The transmembrane domain is underlined; peptide sequences identified by mass spectrometry sequencing are highlighted in bold. (**E** and **F**) Distribution of αGalCer in FAAH-deficient serum (**E**) assessed after gel filtration chromatography, as described in **A**, and in serum protein fractions after anion exchange chromatography (**F**), performed as described in **B**.

animals exhibit an antiinflammatory phenotype, which can in some instances be attributed to signaling via CB receptors (31, 32) but otherwise is independent of the endocannabinoid system (27, 33, 34).

Here we have screened the murine serum proteome and identified FAAH as an αGalCer-binding protein that modulates NKT cell activation in vivo. Deficiency in FAAH resulted in a dysregulation of NKT cell activation characterized by a decreased systemic cytokine production and enhanced proliferation of NKT cells in response to αGalCer stimulation. Surprisingly, this phenotype was not linked to absence of cellular FAAH or enhanced CB receptor signaling, but rather resulted from the altered serum transport and uptake of αGalCer for presentation via CD1d. Thus, our results demonstrate the presence and previously unknown function of FAAH in normal mouse serum. Moreover, these findings identify an important role for the serum protein transport of glycolipid antigens in the induction of key effector functions of NKT cells.

Results

Identification of FAAH as an αGalCer-binding protein in serum

To examine the transport of lipid antigens, we studied the serum distribution of the prototypic NKT cell agonist αGalCer (35) by using gel filtration and anion exchange chromatography in combination with mass spectrometry identification. We chose αGalCer as a model antigen because of its importance for human clinical trials. In addition, initial experiments revealed that αGalCer was still efficiently CD1d presented by *Ldlr*-deficient APCs (Supplemental Figure 1A; supplemental material available online with this article; doi:10.1172/JCI40451DS1), which suggested that serum proteins other than apoE (25) contributed to the transport and cellular uptake of αGalCer in vivo. C57BL/6 mice were injected with 1 μg αGalCer i.v., and serum was collected at various times after injection. The presence of an NKT cell stimulatory activity in the serum was detected in a biological assay using the DN32.D3 NKT cell hybridoma as a reporter in an antigen presentation assay. Preliminary experiments indicated that, after injection, most of the stimulatory activity was cleared from circulation within 30–60 minutes, presumably via uptake by the liver, to reappear progressively after 2 hours and peak between 2 and 4 hours (Supplemental Figure 1B). In subsequent experiments serum was therefore collected after 3 hours for fractionation and detection of the stimulatory activity in individual fractions. After gel filtration, αGalCer activity was detected in association with VLDL, LDL, and HDL as well as in fractions containing the pool of serum proteins, thus indicating that αGalCer was transported by both lipoprotein particles and serum proteins (Figure 1A). Further separation of the pooled serum protein fractions by anion exchange chromatography yielded 3 major peaks eluting at 150 mM, 240 mM, and 270 mM salt. Most bioactivity co-eluted with the third peak (Figure 1B). Only two fractions of this elution peak contained

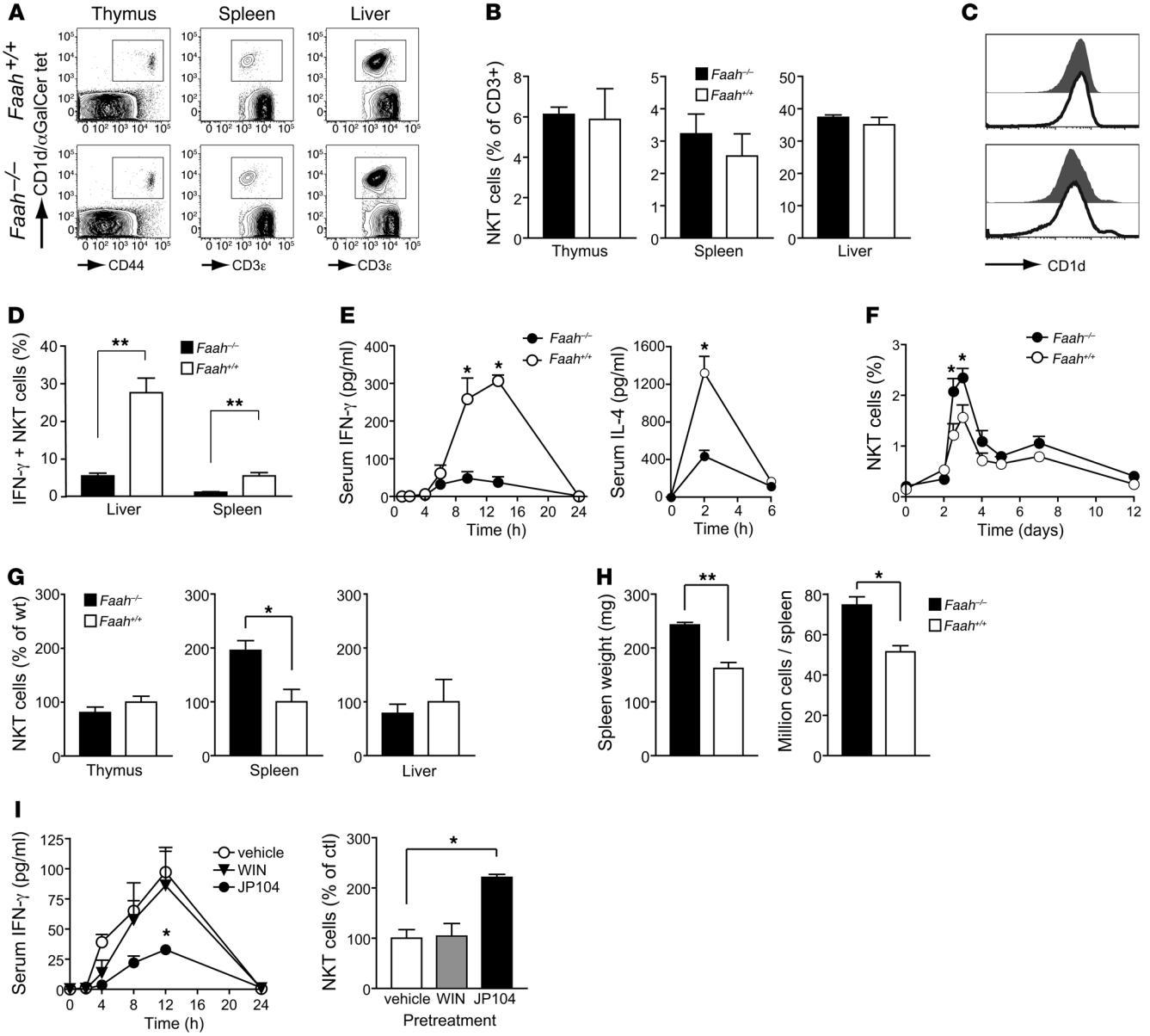

Figure 2

Aberrant NKT cell activation in *Faah*-deficient mice. (**A** and **B**) NKT cell populations in thymus, spleen, and liver of naive WT and *Faah* KO mice. Data of individual mice is shown in **A** and means ± SD of groups of 3 mice from 1 of 3 similar experiments in **B**. (**C**) CD1d expression on thymocytes (top panel) and splenocytes (bottom panel) of *Faah* KO (white histogram) and WT (gray histogram) mice as determined by flow cytometry. (**D**) Decreased induction of IFN-producing NKT cells in livers and spleens of *Faah* KO mice 1 hour after injection of 1 μg αGalCer. (**E** and **F**) Serum cytokine levels (**E**) and expansion of NKT cells (**F**) in blood of *Faah* KO and WT mice in response to αGalCer injection. (**G** and **H**) NKT cell expansion in thymus, liver, and spleen (**G**), and splenic weight and cell numbers (**H**) of αGalCer-immunized *Faah* KO and WT mice at day 3 after immunization with αGalCer. (**I**) Decreased systemic cytokine production and enhanced NKT cell expansion depends on FAAH protein but is independent of CB signaling. WT mice were pretreated with FAAH inhibitor JP104, CB1/2 receptor mimetic WIN 55212-2, or vehicle before i.v. immunization with αGalCer. Data (mean ± SEM) are representative of 2 experiments with 3 mice per group (**D**, **E**, and **I**) or 4 mice per group (**F**), and of 3 experiments with 3 mice per group (**G** and **H**).

a high specific stimulatory activity when normalized for total protein concentration. SDS-PAGE analysis revealed a few major protein bands between 70 kDa and 150 kDa of apparent molecular size in the fractions with high specific activity (Figure 1C). The bands were excised, digested with trypsin, and subjected to mass spectrometry for identification. Six peptides of FAAH (Figure 1D and Supplemental Figure 2A) and 15 peptides of complement precursor 3b (Supplemental Figure 2B) were identified by mass spectrometry sequencing as the most abundant proteins corresponding to the 70 kDa and 150 kDa bands, respectively. The direct binding of C3 to lipids has been previously demonstrated (36), but when we examined the distribution of αGalCer in the serum of *C3*-deficient mice, it was indistinguishable from that of WT serum (Supplemental Figure 2C). Therefore, a primary role of C3 in the transport of αGalCer was unlikely,

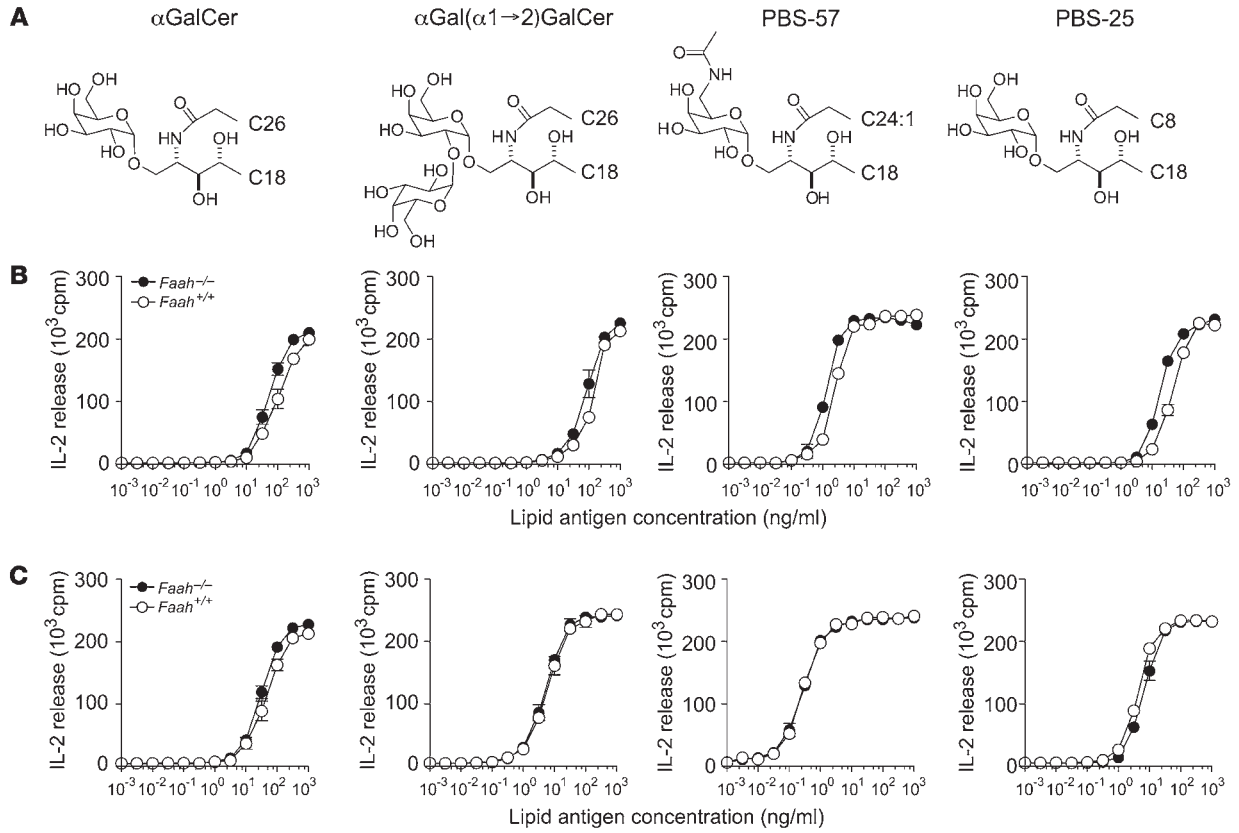

Figure 3
Cellular expression of FAAH is dispensable for CD1d antigen presentation. (**A**–**C**) Presentation of the NKT cell agonists (**A**) to DN32.D3 hybridoma cells by splenic APCs (**B**) and by bone marrow-derived DCs (**C**) from *Faah* KO (black circles) and WT (white circles) mice. Data represent mean ± SD of triplicate measurements from 1 of 2 similar experiments.

and this line of investigation was not pursued further. On the other hand, FAAH-deficient serum almost completely lacked the stimulatory activity in the corresponding serum fractions (Figure 1, E and F). In addition, FAAH-deficient serum also showed reduced amounts of αGalCer bound to the VLDL, LDL, and HDL fractions. Taken together, these data demonstrated that FAAH was present in normal mouse serum and suggested that FAAH bound αGalCer. Furthermore, they indicated that FAAH might contribute to the transfer of lipid antigens onto lipoprotein particles and to the dynamics of transport of αGalCer in serum and immunological sites.

Dysregulation of NKT cell responses in Faah-deficient mice

In order to evaluate the potential role of FAAH in NKT cell biology we next examined NKT cell responses in *Faah*-deficient animals. Naive *Faah*-deficient mice had normal NKT cell numbers in thymus and liver, but slightly more NKT cells in spleen (Figure 2, A and B). Absence of FAAH did not influence the populations of conventional T cells (Supplemental Figure 3A), and *Faah* KO and WT mice showed similar levels of CD1d expression on thymic and splenic APCs (Figure 2C). Thus, except for a trend toward increased splenic NKT cell numbers, naive *Faah*-deficient mice exhibited normal T cell populations. However, *Faah*-deficient mice produced drastically less IFN-γ and IL-4 after injection of αGalCer, as assessed by the percentage of cytokine-producing NKT cells (Figure 2D) and the cytokine concentration in serum (Figure 2E). Paradoxically, despite this reduced cytokine response to αGalCer, *Faah*-deficient mice exhibited an increased expansion of NKT cells in blood (Figure 2F). While livers and thymi of *Faah*-deficient mice contained WT levels of NKT cells at day 3 after injection, the splenic NKT cell population expanded in *Faah* KO mice to up to 200% of WT numbers (Figure 2G). The unusual NKT cell response to αGalCer injection was accompanied by a 50% increase in splenic weight and cellularity in *Faah* KO mice as compared with WT animals (Figure 2H). This was attributable to higher numbers of $CD4^+$ and $CD8^+$ T cells and of B cells, although the relative increase of these lymphocyte subsets in *Faah*-deficient mice was less pronounced than that of NKT cells (Supplemental Figure 3B).

Since FAAH degrades endogenous fatty acid amides and *Faah*-deficient mice accumulate higher levels of endocannabinoids (30), we next evaluated whether the observed NKT cell phenotype resulted from increased endocannabinoid signaling or from the absence of FAAH protein. WT C57BL/6 mice were treated with the irreversible FAAH inhibitor JP104 (37) or with the cannabinomimetic WIN 55212-2 (38). Mice were then injected with αGalCer, and the cytokine responses in serum and NKT cell expansion in organs were compared with those of αGalCer-injected, vehicle-treated controls. While deliberate triggering of CB receptors affected neither the cytokine production nor expansion of NKT cells, the phenotype of *Faah*-deficient mice was reproduced in WT mice by chemical ablation of FAAH activity (Figure 2I). We therefore concluded that the dysregulated NKT cell responses observed in *Faah* KO mice were not related to increased CB receptor signaling (39), but directly linked to a function of FAAH in CD1d antigen presentation and NKT cell activation.

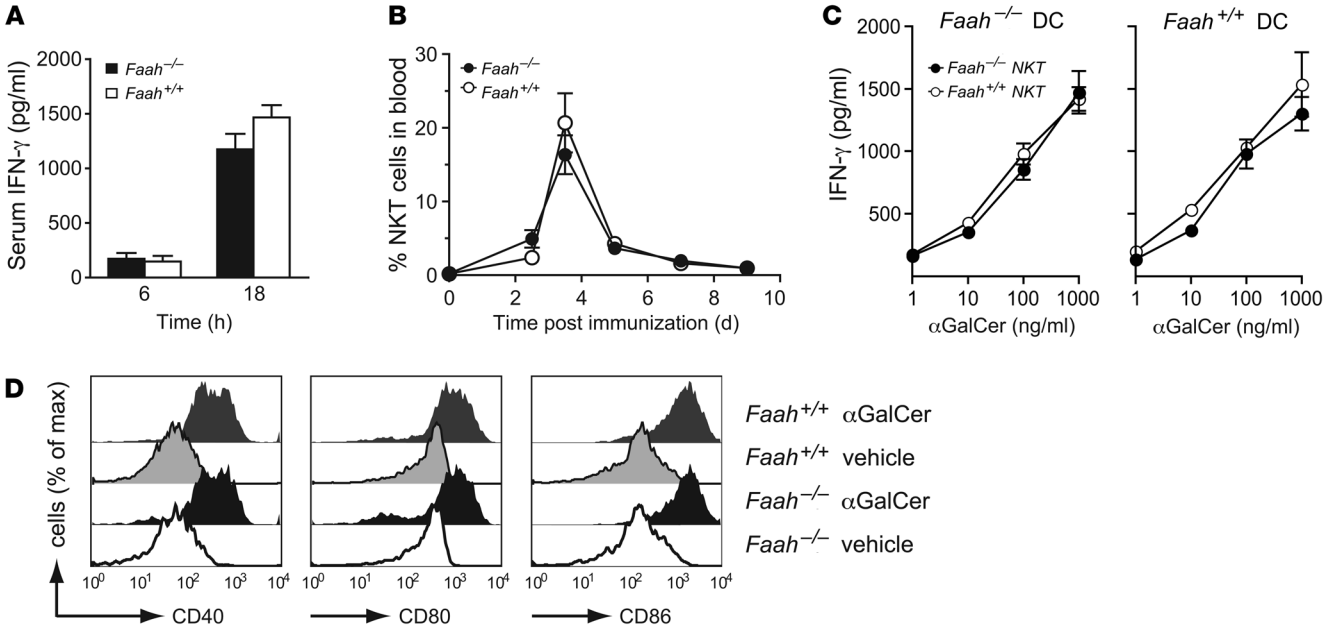

Figure 4
Cellular expression of FAAH is dispensable for physiological NKT cell function. (**A** and **B**) In vivo responses of *Faah* KO and WT NKT cells to immunization with lipid antigen–pulsed WT DCs were assessed at the indicated times by IFN-γ production in serum (**A**) and expansion of NKT cells in blood (**B**). (**C**) In vitro stimulation of splenic NKT cells from *Faah* KO and WT mice with either lipid-pulsed KO or WT DCs resulted in normal IFN-γ production. Data in **A**–**C** are presented as the mean ± SEM. (**D**) Comparable induction of NKT cell–dependent DC maturation in response to αGalCer stimulation in vivo. WT and *Faah* KO mice were injected with 1 μg αGalCer i.v., and 18 hours later the expression of DC maturation markers CD40, CD80, and CD86 was assessed on splenic CD11c+ cells by flow cytometry.

Defect in NKT cell activation is not caused by absence of cellular FAAH

Antigen presentation. To elucidate the mechanism underlying the altered NKT cell responses associated with *Faah* deficiency, we first tested the ability of *Faah*-deficient APCs to present lipid antigens to the NKT cell hybridoma DN32.D3 in vitro (Figure 3). *Faah*-deficient splenocytes (Figure 3B) and bone marrow–derived DCs (Figure 3C) presented αGalCer equally well as WT APCs. The fact that *Faah*-deficient APCs also presented the digalactosylceramide αGalCer(α1→2)GalCer (PBS-18), which requires lysosomal processing of the terminal galactose in order to activate NKT cells (40), suggested that the absence of cellular FAAH did not impair the uptake and processing of glycosphingolipid antigens. In addition, both PBS-57, an optimized αGalCer variant with higher stability (41), and PBS-25, an αGalCer variant with shortened acyl chain (42), were presented equally well in the absence of cellular FAAH expression.

NKT cell responses. We next assessed whether expression of FAAH by NKT cells was required for normal NKT cell responses. To avoid potential defects in CD1d antigen presentation in vivo in the *Faah* KO animals, NKT cell responses of WT and KO mice were examined after priming with in vitro αGalCer-pulsed WT DCs. In contrast to the reduced cytokine production seen after immunization with soluble lipid antigen, *Faah* KO mice responded with WT levels of IFN-γ to priming with αGalCer-pulsed DCs (Figure 4A) and showed an equal expansion of NKT cells (Figure 4B). Furthermore, *Faah*-deficient NKT cells also produced WT levels of IFN-γ when stimulated with lipid-pulsed WT or KO DCs in vitro (Figure 4C).

DC/NKT cell interaction. Since these experiments revealed no defects in CD1d antigen presentation or NKT cell function in the absence of cellular FAAH expression, we investigated whether the cooperation between NKT cells and DCs was altered in vivo in *Faah* KO mice. *Faah*-deficient and WT mice were injected with αGalCer, and 18 hours later the NKT cell–induced maturation of splenic DCs was assessed by flow cytometry. Both KO and WT mice exhibited a comparable upregulation of costimulatory molecules CD80, CD86, and CD40 on splenic DCs upon injection of αGalCer, indicating a similar degree of DC maturation in both mouse strains (Figure 4D). Thus, neither cellular function per se nor the interaction between DCs and NKT cells was defective in the absence of cellular FAAH expression.

Serum FAAH regulates delivery of lipid antigen toward CD1d antigen presentation

Given the normal phenotype of *Faah*-deficient APCs and NKT cells, the dysregulation of NKT cell responses observed in *Faah* KO animals could only be explained by a defective transport and/or uptake of lipid antigen. To directly address this issue, NKT cell stimulation assays were repeated without FCS, a potential source of FAAH or FAAH-like activity. Splenic APCs were pulsed with lipids in the presence of WT or FAAH-deficient murine serum and used to stimulate NKT cell hybridoma cells. Both WT and *Faah*-deficient APCs presented αGalCer equally well when pulsed in the presence of WT serum (Figure 5A). Strikingly, the CD1d presentation of αGalCer was severely reduced when APCs were pulsed in the presence of FAAH-deficient serum, irrespective of the ability of the APCs to express FAAH (Figure 5A). Complementing these

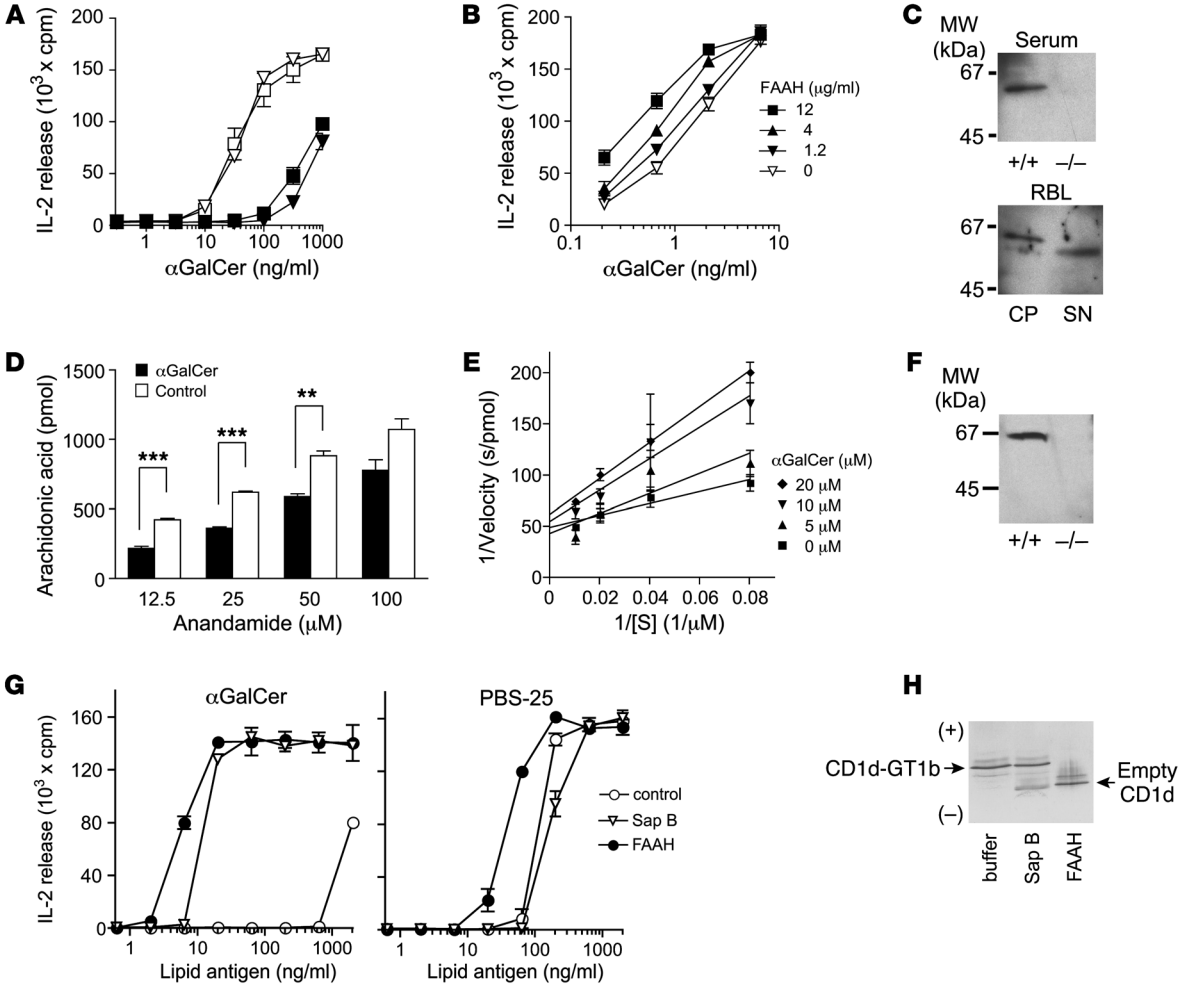

Figure 5

FAAH is required in serum for the efficient CD1d presentation of exogenous lipid antigen, binds directly to GalCer, and modifies the lipid content of CD1d. (**A**) Stimulation of DN32.D3 cells with *Faah* KO (triangles) and WT splenocytes (squares) pulsed with lipid antigen in the presence of FAAH-deficient (black symbols) or FAAH-containing (white symbols) mouse serum. (**B**) CD1d presentation of αGalCer to DN32.D3 cells by WT DCs in the presence of exogenous recombinant FAAH. (**C**) Presence of FAAH in murine serum and in supernatant of RBL cells. Immunoprecipitation of WT serum, *Faah* KO serum, RBL cell pellets (CPs), and RBL cultured supernatant (SN) with an anti-FAAH mAb, and detection by immunoblot analysis. (**D** and **E**) αGalCer inhibits hydrolysis of anandamide by recombinant FAAH protein. (**D**) Enzymatic activity in the absence (white bars) and presence (black bars) of 25 μM αGalCer. (**E**) The apparent K_m values were calculated for inhibition assays performed at the indicated αGalCer concentrations and plotted against the inhibitor concentration to calculate the inhibitor binding constant (K_i). (**F**) Precipitation of FAAH from liver cell lysates of WT mice but not *Faah*-deficient mice with a modified biotinylated αGalCer variant. (**G** and **H**) FAAH-mediated glycolipid transfer to, and extraction from, CD1d. (**G**) Loading of αGalCer and PBS-25 into plate-bound CD1d in the presence of FAAH or saposin B (Sap B) or without lipid transfer protein (LTP) (control) was assessed by DN32.D3 hybridoma cell stimulation. (**H**) Unloading of prebound ganglioside GT1b from CD1d by FAAH and saposin B as analyzed by isoelectric focusing gel electrophoresis. Plotted data represent the mean ± SEM.

results, the addition of exogenous recombinant FAAH protein enhanced the CD1d presentation of αGalCer by WT APCs, especially at limiting lipid concentrations (Figure 5B). Thus, CD1d antigen presentation was independent of cellular FAAH expression but critically required the presence of extracellular, serum-derived FAAH protein. We therefore sought direct evidence for the presence of FAAH in serum using a novel monoclonal anti-FAAH antibody. FAAH protein was immunoprecipitated from serum of WT but not *Faah* KO mice and from culture supernatant of rat basophilic leukemia (RBL) cells, which express high levels of endogenous FAAH (Figure 5C). Compared with the cell-associated FAAH that precipitated from RBL cell extracts, serum-derived and RBL cell–secreted FAAH was slightly smaller in size, possibly indicating that a processed form of FAAH was released from cells and into extracellular media.

Direct binding of αGalCer to FAAH

Since these data suggested a role of FAAH in the transport and targeting of lipid antigens for CD1d presentation and since we co-isolated αGalCer with FAAH from serum (Figure 1), we next investigated a potential direct interaction between FAAH and αGalCer. Co-incubation of αGalCer with increasing amounts

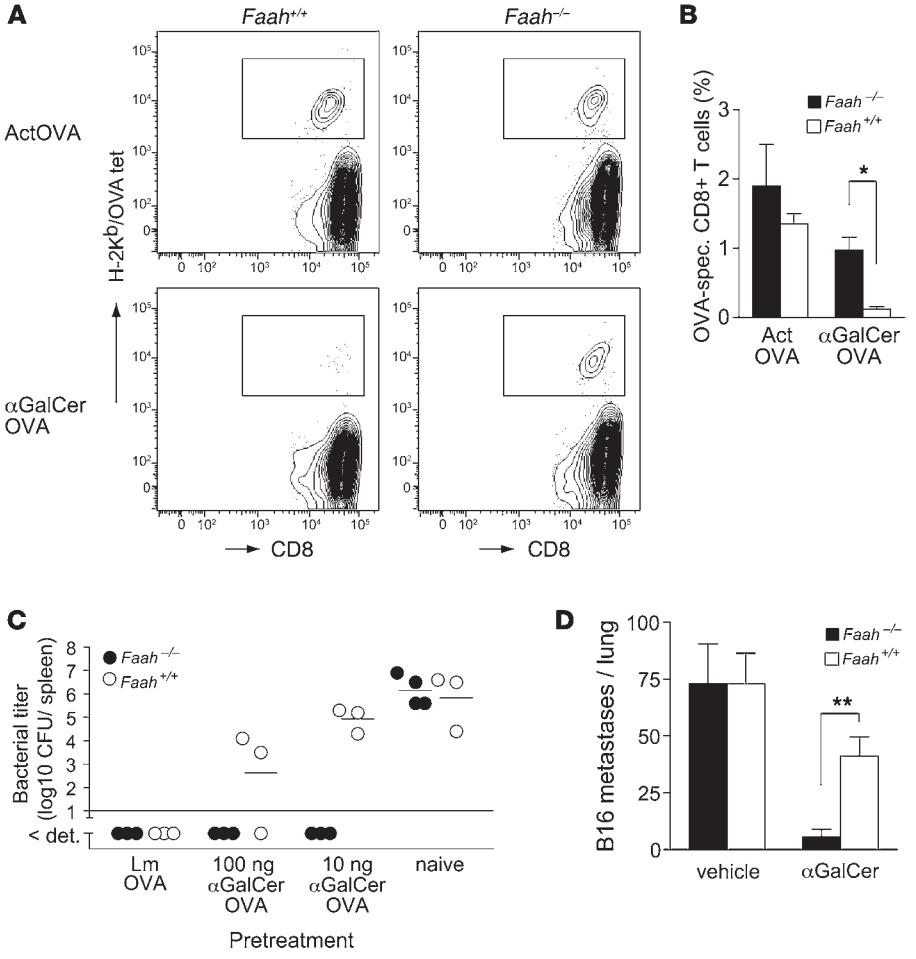

Figure 6
NKT cell activation in the absence of FAAH enhances the priming of CTL responses and protects mice against B16 melanoma metastasis. (**A** and **B**) Expansion of ovalbumin-specific CD8+ T cell responses after immunization with ovalbumin-expressing splenocytes (ActOVA) or with ovalbumin protein and αGalCer (αGalCer OVA). FACS profiles of individual mice are shown in **A** and means ± SD of groups of 3 mice in **B**. (**C**) Bacterial titers in spleens of individual *Faah*-deficient (black circles) and WT (white circles) mice 3 days after challenge with 1×10^5 CFU LmOVA. Data represent 1 of 2 similar experiments with 3 to 4 mice per group. (**D**) Number of melanoma lung metastases in αGalCer-treated WT and *Faah* KO mice 14 days after i.v. inoculation with 2×10^5 B16F10 cells. Means ± SD of groups of 4 mice from 1 of 2 similar experiments are shown.

of recombinant FAAH monitored by LC-MS did not reveal any degradation of αGalCer by recombinant FAAH in vitro. However, αGalCer competed with the physiological FAAH substrates for binding to FAAH and inhibited the hydrolysis of oleamide (data not shown) and of anandamide in a dose-dependent manner (Figure 5D). The K_i of the interaction was calculated at 16 ± 4 μM (Figure 5E) and was thus very close to that of natural substrates (27). Moreover, the ability of a modified, biotinylated αGalCer variant to pull-down cellular FAAH from liver lysate of WT but not *Faah* KO mice provided further evidence for the direct binding of αGalCer by FAAH (Figure 5F).

FAAH loads αGalCer into CD1d and extracts bound glycolipid from CD1d

Our data indicated that FAAH binds αGalCer and is required in serum for the efficient targeting of αGalCer for CD1d presentation. We therefore evaluated the ability of FAAH protein to enhance CD1d presentation in the absence of other serum-derived or cell-secreted factors. Direct loading of isolated αGalCer into plate-bound CD1d molecules is very inefficient and was observed only at very high concentrations of antigen (Figure 5G). However, recombinant FAAH strongly enhanced the loading of αGalCer into CD1d by several orders of magnitude (Figure 5G). This lipid transfer activity of FAAH was equivalent to that of the lysosomal lipid transfer protein saposin B. In comparison, the loading of an αGalCer variant with shortened acyl chain (PBS-25) did not depend on lipid transfer proteins, but was also slightly enhanced in the presence of FAAH (Figure 5G). Furthermore, recombinant FAAH also unloaded bound ganglioside GT1b from CD1d at least as efficiently as saposin B (Figure 5H). Taken together, these in vitro findings illustrated that FAAH can function as a lipid transfer protein that has the ability to modify the lipid content of CD1d.

NKT cell activation in the absence of FAAH supports the priming of antimicrobial CD8+ T cell responses and confers enhanced protection against B16 metastasis

It appeared from our results that direct binding of αGalCer to FAAH is a critical step for the normal NKT cell response to lipid antigens. We therefore tested the influence of FAAH on CD8+ T cell priming against a nominal antigen, e.g., ovalbumin, using NKT cell activation as an adjuvant. Priming with ovalbumin peptide–expressing splenocytes induced a comparable expansion of ovalbumin-specific CTLs in both *Faah* KO and WT mice (Figure 6, A and B), excluding intrinsic defects in the *Faah* KO mice that might affect the priming and expansion of ovalbumin-specific CTL. However, upon immunization with a suboptimal priming dose of ovalbumin using αGalCer as an adjuvant, the enhanced expansion of NKT cells led to the priming of strong ovalbumin-specific CTL responses in *Faah*-deficient mice, whereas a similar immunization induced only weak CD8+ T cell responses in WT mice (Figure 6A).

Compared with WT controls, priming with ovalbumin and αGalCer resulted in an approximately 8-fold higher CTL expansion in *Faah* KO mice (Figure 6B). This enhanced $CD8^+$ T cell priming also conferred increased protection from infection with *Listeria monocytogenes* (Figure 6C). Immunized mice were challenged with 10^5 CFU of *Listeria*-expressing recombinant ovalbumin (LmOVA; ref. 43), and *Listeria* titers were assessed in spleens (Figure 6C) and livers (Supplemental Figure 5) 3 days later. The bacterial burden was comparable in organs of infected non-immunized *Faah* KO and WT mice, suggesting that deficiency in FAAH did not alter the susceptibility to *Listeria* infection. Although the immunization with ovalbumin and 100 ng αGalCer protected *Faah* KO mice almost as well as a previous infection with LmOVA, it clearly conferred much weaker protection in WT mice (Figure 6C). Moreover, while immunization of *Faah*-deficient mice with a 10-fold lower dose of lipid adjuvant was still sufficient to control *Listeria* completely in spleen (Figure 6C) and to reduce the bacterial titers in livers by 3 orders of magnitude (Supplemental Figure 5), such protection was not observed in similarly immunized WT mice (Figure 6C and Supplemental Figure 5). Taken together, these results demonstrated that NKT cell activation in the absence of FAAH conveys an enhanced adjuvant effect for the priming of protective $CD8^+$ T cell responses.

We next evaluated the ability of WT and *Faah*-deficient mice to control a high dose B16 melanoma challenge. Vehicle-treated *Faah* KO and WT mice exhibited similar lung metastasis 14 days after inoculation, which indicated a comparable susceptibility to tumor metastasis in *Faah*-deficient and WT mice (Figure 6D). However, while αGalCer-treated *Faah* KO mice almost completely controlled the tumor challenge (5.6 ± 3.4 vs. 73.0 ± 24.8 foci in the αGalCer vs. vehicle groups), similarly treated WT mice exhibited only a 50% reduction in the number of lung metastases as compared with vehicle-treated controls (41.2 ± 14.6 vs. 72.9 ± 27.2 foci in the αGalCer vs. vehicle groups; Figure 6D). Since the anti-metastatic activity of individual NKT cell subsets differs greatly (24), we further characterized the NKT cell subpopulations in WT and *Faah*-deficient mice according to cell surface expression of NK1.1 and CD4 (Supplemental Figure 4, A and B). Consistent with their higher resistance to melanoma metastasis, naive *Faah*-deficient mice had an increased proportion of double-negative (DN) liver NKT cells (Supplemental Figure 4B), the subset that imparts most of the anti-metastatic activity of αGalCer treatment (24). A higher proportion of DN NKT cells was also present in livers and spleens of *Faah* KO mice after αGalCer injection (Supplemental Figure 4C). Thus, activation in the absence of FAAH enhanced the ability of NKT cells to protect from B16 melanoma, which correlated with a larger population of DN NKT cells present in *Faah*-deficient mice.

Absence of FAAH differentially affects individual NKT cell functions

Collectively, our results indicated that FAAH modulated the transport, targeting, and possibly CD1 loading/unloading of αGalCer and thereby modified its CD1 presentation. It was rather unexpected that the effector responses of NKT cells were not uniformly reduced in *Faah* KO mice — as observed for the cytokine production — but that some aspects of the natural NKT cell responses to αGalCer were actually enhanced in the absence of FAAH. To examine whether this was related to an altered CD1 presentation in the absence of FAAH in vivo, we next assessed the ex vivo antigen presentation by splenic and hepatic DCs isolated from αGalCer-injected WT and *Faah*-deficient mice. Hepatic DCs isolated from *Faah* KO mice stimulated the NKT cell hybridoma approximately 10-fold better than WT DCs, whereas DCs isolated from spleens of *Faah* KO and WT mice showed no difference (Supplemental Figure 6). Hence, the absence of FAAH affected the targeting of αGalCer to DCs in vivo differently depending on the organ and increased the uptake of αGalCer by hepatic DCs.

Since individual NKT cell functions may vary in their sensitivity to the strength of the antigenic stimulus, and consequently also may differ in their requirement of FAAH, we compared NKT cell–produced cytokine and NKT cell–induced DC maturation in response to titrated amounts of αGalCer in WT and *Faah* KO mice. While a clear effect of FAAH on the cytokine response was seen at all lipid antigen doses tested, the requirement of FAAH for the NKT cell–induced DC maturation only became apparent at limiting doses of antigen (Supplemental Figure 7). Thus, the induction of DC maturation was less sensitive to antigenic potency than the NKT cell cytokine response, and therefore depended less on efficient lipid loading by FAAH. In summary, FAAH appears to modulate the in vivo bioactivity of αGalCer via its serum transport, cellular targeting, and direct interference with loading onto CD1d. As a result, individual effector functions of NKT cells seem to be differentially affected by FAAH deficiency.

Discussion

NKT cells serve as a powerful adjuvant of natural immune responses; hence NKT cell agonists are emerging as promising candidates for novel vaccination strategies. Although first clinical trials using NKT cell agonists in the immunotherapy of cancer are already being conducted, our knowledge about the in vivo properties of such lipid antigens and factors that control their bioactivity is still very limited. Here we have isolated the enzyme FAAH as an αGalCer-binding serum protein that differentially modulates cytokine production and expansion of NKT cells in vivo. NKT cell activation in the absence of FAAH resulted in an enhanced proliferation of splenic NKT cells and drastically augmented the efficacy of αGalCer to promote the priming of protective $CD8^+$ T cells. Thus, the interaction of lipid antigens with serum proteins directly regulates the induction of key effector functions of NKT cells and may potentially be targeted in order to enhance the NKT cell–mediated adjuvant effect.

Two classes of lipid-binding proteins mediate the serum transport of endogenous and microbial lipids. First, lipids are transported by lipoproteins, specialized lipid carrier vehicles, which can be distinguished by their density, lipid composition, and associated apolipoproteins. Apolipoproteins facilitate the solubility of the lipid cargo, control the binding and exchange of lipids, and target the lipoprotein particle to uptake via specific cell surface receptors. The second class of proteins, termed serum lipid transfer proteins, regulates the lipoprotein-mediated transport by transferring lipids onto and between lipoproteins, assisting in lipid processing, or directing lipids to lipoprotein-independent uptake pathways. For example, while binding to LPS-binding protein targets bacterial LPS for TLR4 recognition (44), the association of LPS with lipoproteins rather results in uptake and detoxification of LPS by hepatocytes, thereby limiting the potentially adverse effects of TLR signaling (45). Thus, the binding of lipid antigens to lipoproteins or serum lipid transfer proteins regulates the immune recognition of lipid antigens and modulates the resulting immune response.

Recently, a pivotal role of the VLDL fraction for targeting of lipid antigens toward CD1 presentation was proposed (25). The VLDL-associated apoE was shown to mediate the uptake of digalactosylceramide via the LDLR, which resulted in delivery of this lipid to the lysosome for processing and loading onto CD1d. Interestingly, compared with digalactosylceramide (PBS-18), we found αGalCer to depend much less on LDLR-mediated uptake, as αGalCer was still efficiently presented by *Ldlr* KO APCs, whereas PBS-18 was not (Supplemental Figure 1A). Since this suggested that the cellular uptake of αGalCer was not exclusively mediated via the apoE/LDLR pathway, it prompted us to search for other serum factors involved in the CD1d presentation of αGalCer. We detected αGalCer in both the major serum lipoprotein fractions as well as the pool of soluble serum proteins. It appears from our results that FAAH represents the main soluble serum protein involved in the serum transport of αGalCer. FAAH bound αGalCer in vitro (Figure 5, D–F) and co-fractionated with the stimulatory activity from murine serum (Figure 1B). The lack of stimulatory activity in the respective serum fractions of FAAH-deficient serum strongly suggested that in WT serum FAAH is responsible for the association of αGalCer with these serum fractions, where αGalCer most likely is present in complex with FAAH. At the same time, we observed that in FAAH-deficient serum, reduced amounts of αGalCer were present in the lipoprotein fractions, indicating that FAAH might also contribute to the transfer of αGalCer onto lipoprotein particles (Figure 1E). We can only speculate which cell surface receptor is involved in the cellular uptake of αGalCer for CD1d presentation. While our experiments using *Ldlr*-deficient APCs excluded an important role of the LDLR (Supplemental Figure 1A), preliminary results also seem to rule out an involvement of the class B scavenger receptors SRB1 and CD36 (data not shown). Nevertheless, we observed a partial reduction in CD1d presentation of αGalCer by scavenger receptor A–deficient APCs (S. Freigang and L. Teyton, unpublished observations). To what extent this receptor-mediated uptake of αGalCer implies direct binding and uptake of αGalCer/FAAH complexes or rather requires FAAH-mediated transfer of αGalCer onto lipoproteins remains to be investigated. However, the drastically reduced presentation of αGalCer in absence of serum-derived FAAH in vitro and the enhanced CD1d presentation in the presence of recombinant FAAH suggest that extracellular FAAH is critically involved in both transport and uptake of αGalCer.

FAAH is an integral membrane protein located in the ER and has not yet been described as an extracellular protein. Structural and biochemical studies suggest that FAAH remains membrane associated even after deletion of its transmembrane domain, presumably because of structural adaptations that are absent from related, soluble enzymes of the amidase signature protein family (27, 29). Hence, it seemed most unusual that we purified FAAH from murine serum as an αGalCer-binding protein. Nevertheless, 6 different peptides that we isolated from mouse serum unequivocally identified murine FAAH. How can this be explained? The serum proteome is currently a subject of intensive research, and several reports have now consistently shown that 30% to 50% of the identified serum proteome are intracellular proteins without a known secretion pathway (46, 47). Therefore, even the absence of a known mechanism may not preclude that FAAH is released into serum where it modulates the transport of lipid antigens. Given the importance of fatty acid amide signaling, FAAH is an evolutionary conserved protein, and homolog enzymes have also been identified in invertebrates and protozoa. Interestingly, the unicellular parasite of fish, *Tetrahymena pyriformis*, expresses a secreted form of FAAH that cross-reacts with antibodies specific for rat FAAH (48, 49). Although the sequence homology and secretion mechanism for the FAAH of *T. pyriformis* are still unknown, it is tempting to speculate that a similar, yet unidentified pathway may be involved in the secretion of murine FAAH into serum. Indeed, the FAAH protein that we immunoprecipitated from serum and from supernatant of FAAH-expressing cells was of reduced molecular weight, suggesting that a processed form of cellular FAAH may be released from cells and into serum. The mechanism of FAAH secretion and its potential regulation in infections and inflammatory conditions will certainly merit further investigation.

The aberrant NKT cell phenotype observed in *Faah*-deficient mice exposes 2 aspects of NKT cell activation that seem to be modulated by FAAH. First, αGalCer stimulation in the absence of FAAH led to a dissociation of the NKT cell responses at different sites, e.g., normal proliferation in liver and thymus, but an enhanced NKT cell expansion of the splenic NKT cell population after systemic application of αGalCer. Second, FAAH deficiency also influenced the quality of the induced cellular response. The reduced systemic IFN-γ and IL-4 response in *Faah*-deficient mice was contrasted by an increased adjuvant effect and anti-metastatic activity of NKT cell activation. The reciprocal dysregulation of these effector functions in *Faah*-deficient mice may seem paradoxical since IFN-γ production by NKT cells has been shown to be required for both the adjuvant and the anti-metastatic activity of αGalCer immunization. For example, adoptive transfer experiments indicate a requirement for NKT cell–produced IFN-γ for tumor rejection (50). However, CD4-negative liver-resident NKT cells were later identified as the main mediators of tumor rejection in this model, although this particular subset did not differ from the other NKT cell subsets in the level of IFN-γ produced (24). We found an increased proportion of $CD4^-$ NKT cells in livers of naive and αGalCer-injected *Faah* KO mice, which might have contributed to the better melanoma control in these mice. Importantly, the IFN-γ response was reduced but not completely abrogated in the absence of FAAH and may have sufficed to ensure the necessary IFN-γ signaling.

Our findings also provide important mechanistic insight into how FAAH modulates CD1d presentation that may explain the dissociation of individual NKT cell responses in the KO. It appears that FAAH binds αGalCer in serum (Figures 1 and 5) and can regulate its loading onto CD1d molecules in vitro (Figure 5). The uptake and intracellular trafficking of lipid/FAAH complexes will have to be examined closely to evaluate the in vivo consequences of these observations. At the present time, it is reasonable to assume that FAAH modifies the bioavailability of αGalCer for CD1d presentation, especially in the liver. The reduced cytokine response in *Faah*-deficient mice might indicate that the absence of serum FAAH limits the kinetics of αGalCer entering the CD1d pathway, which in turn impairs the NKT cell cytokine response. While the requirement of FAAH for the cytokine response was seen at all lipid antigen doses, the NKT cell–induced DC maturation was clearly less dependent on the presence of FAAH, suggesting that various aspects of the αGalCer response are differentially regulated and affected by the presence or absence of particular lipid transporters/exchangers. Along the same lines, the present data clearly established that cytokine secretion and expansion of NKT cells in blood and spleen were dissociated. Therefore, in practical terms, it would be reasonable to associate the enhanced adjuvant effect of NKT cell activation in *Faah* KO mice with the phenotype of

hepatic DCs and the NKT cellular expansion, and to suggest that systemic cytokine secretion is a poor parameter to predict the adjuvant power of a given NKT cell agonist. Moreover, the increased targeting of αGalCer to liver DCs in *Faah* KO mice (Supplemental Figure 6) also underscores the organ-to-organ differences in NKT cell biology and could simply be related to the quantities of FAAH present in different tissues (liver and brain are the organs in which FAAH is the most abundant). In this context, it is interesting to mention that hepatic DCs have recently been shown to predominantly mediate the adjuvant effect of αGalCer vaccination (51). In summary, FAAH seems to balance the individual NKT cell effector functions like a rheostat of NKT cell activation. On one hand, efficient loading of αGalCer into CD1d may be essential to guarantee the physiological cytokine response. On the other hand, the interaction of αGalCer with FAAH appears to limit its uptake by hepatic DCs or to favor a nonproductive pathway (degradation or absence of intersection with CD1d) and at the same time to constrain the enhanced splenic NKT cell expansion and increased adjuvant effect that was observed in *Faah* KO mice.

In conclusion, our results indicate that by binding αGalCer in serum, FAAH modulates its transport and targeting for CD1d presentation, which subsequently results in a differential activation of individual NKT cell subsets and effector functions. Importantly, the ability of a given lipid antigen to bind different serum (lipo)proteins is determined by its chemical structure. Our findings therefore imply that structural modifications of lipid antigens that increase or decrease their binding to serum proteins, such as FAAH or apoE, could prove useful in order to achieve an organ-specific activation of NKT cell subsets or the selective induction of certain NKT cell effector functions in vivo. Given that αGalCer is still the only NKT cell agonist used in clinical trials, the identification of FAAH has direct clinical implications. Furthermore, it offers a first candidate that could be targeted to provide an enhanced adjuvant effect for the induction of protective $CD8^+$ T cell immunity.

Methods

Antigen presentation assay. CD1d presentation of lipid antigens was detected using the murine NKT cell hybridoma DN32.D3, which expressed the semi-invariant Vα14Jα18/Vβ8 TCR (52). Hybridoma cells were cultured in RPMI supplemented with 10% FCS, 2 mM L-glutamine, 20 mM HEPES, and non-essential amino acids. DCs from WT or *Faah*-deficient mice were generated in in vitro bone marrow cultures (53) in the presence of 2 ng/ml recombinant GM-CSF (Biosource, Invitrogen). DC immunizations were performed with 5×10^5 lipid-pulsed (1 μg αGalCer/ml for 2 hours) DCs per animal. To assess the CD1d presentation by WT and *Faah*-deficient cells, DCs (1×10^4/well) or splenocytes (5×10^5/well) were pulsed with serial dilutions of lipid antigen for 4 hours in 96-well round-bottom plates. For indicated experiments, the lipid pulse was carried out using RPMI supplemented with 5% heat-inactivated murine serum instead of 10% FCS. Cells were then washed 3 times before 5×10^4 DN32.D3 cells were added per well. Supernatant was collected after 24 hours and stored at –80°C until further analysis. The IL-2 concentration in cultured supernatants was determined using $[^3H]$-thymidine incorporation of an IL-2–dependent cell line as a readout. The activation of ex vivo splenic NKT cells was assessed by the production of IFN-γ in response to in vitro stimulation with lipid-pulsed DCs. Cell culture supernatant was harvested 48 hours after stimulation, and IFN-γ concentration was determined with the BD OptEIA Elisa Set (BD Biosciences — Pharmingen).

Isolation of αGalCer-binding proteins from serum. To monitor the serum distribution of NKT cell agonists in vivo, C57BL/6 mice were injected with 1 μg αGalCer i.v., and serum samples were collected at indicated times after injection. Splenocytes of naive C57BL/6 were then pulsed with serial dilutions of serum, and the presence of stimulatory bioactivity was detected using DN32.D3 hybridoma cells as indicators. For further analysis, murine serum was obtained 3 hours after αGalCer injection and fractionated over a HiPrep 16/60 Sephacryl S-300 gel filtration chromatography column (GE Healthcare) using an ÄKTAprime FPLC machine (GE Healthcare). Fractions (0.5 ml) were sterile filtered before the presence of bioactivity was detected by DN32.D3 hybridoma stimulation in vitro. Protein and cholesterol concentrations of individual fractions were determined with the BCA Protein Assay (Pierce Biotechnology) and the Cholesterol Infinity Reagent (Thermo Fisher Scientific) according to the manufacturers' instructions. Fractions containing the soluble serum proteins (corresponding to the elution volume 65–80 ml) were pooled, depleted of albumin overnight by incubation with Blue Sepharose CL-6B (Sigma-Aldrich), and transferred to 50 mM Tris buffer (pH 8.4) by dialysis. The pool of serum proteins was then separated by anion exchange chromatography over a MonoQ HR 16/10 column (GE Healthcare) using a NaCl gradient for protein elution, and fractions (0.5 ml) were tested for bioactivity as described above and analysed by SDS-PAGE. Protein bands from fractions containing stimulatory bioactivity were excised from the gel and digested with trypsin, and proteins were identified by mass spectrometry sequencing analysis at the TSRI core facility.

Mice. *Faah*-deficient mice (30) had been backcrossed for 10 generations onto the C57BL/6 background. *Faah* KO and C57BL/6 WT mice were bred locally at The Scripps Research Institute (TSRI). *Ldlr* KO mice were provided by L. Curtiss (TSRI). All experimental procedures involving animals were performed according to TSRI institutional guidelines and were approved by the TSRI IACUC. Mice were immunized i.v. with titrated amounts of αGalCer, and expansion of NKT cells in blood and organs was assessed by flow cytometry using αGalCer-loaded CD1d tetramers. Ovalbumin-specific $CD8^+$ T cell responses were induced by immunization with 10^7 irradiated ovalbumin-expressing splenocytes, with 200 μg ovalbumin protein in combination with titrated amounts of αGalCer as adjuvant, or with 1,000 CFU LmOVA. On day 8 following immunization, expansion of ovalbumin-peptide–specific $CD8^+$ T cells was assessed by flow cytometry after staining with H2-K^b/SIINFEKL tetramers and by intracellular staining for IFN-γ after restimulation for 5 hours with ovalbumin peptide in vitro.

Reagents. Lipid antigens were synthesized as published previously (41, 42). Lipid stocks (1 mg/ml in dimethylsulfoxide) were diluted to 0.2 mg/ml with PBS containing 0.02% Tween-20. Further dilutions were prepared in PBS for i.v. injections and in cell culture medium for in vitro stimulation assays. JP104 was bought from Cayman Chemical. All other reagents were from Sigma-Aldrich unless otherwise stated. Murine CD1d was produced and loaded with lipid antigen as published (42).

Flow cytometry. NKT cells were quantified in blood and organs using CD1d tetramers loaded with αGalCer. Tetramer and antibody staining was performed on blood collected from the retroorbital plexus, or on single-cell suspensions prepared from spleens, livers, and thymi. Organs were collected in cold PBS, and spleens and thymi were passed through a 70-μm cell strainer to obtain a single-cell solution. Livers were first dissected into small pieces and then passed through a cell strainer before lymphocytes were isolated by Lympholyte M gradient centrifugation (Cedarlane Laboratories Ltd.). Single-cell solutions were treated with Fc Block (BD Biosciences) and 0.5 mg/ml avidin (Sigma-Aldrich) in FACS buffer (FB; PBS containing 2% FCS/2 mM EDTA) at room temperature for 10 minutes. Cells were then washed with FB and stained with CD1d/αGalCer tetramers at room temperature for 15 minutes. Anti-CD3e–APC, anti-B220, or anti-CD44 antibodies (all from BD Biosciences — Pharmingen) were directly added, and staining continued for another 30 minutes. After 2 washes with FB, samples were depleted of erythrocytes and fixed with the BD FACS Lysing Solution (BD Biosciences). Samples were acquired on an LSR II system using the FACSDiva software (both from BD Biosciences) and analyzed with the FlowJo software (Tree Star Inc.).

Expression and purification of FAAH. For in vitro kinetic studies, rat FAAH protein was recombinantly expressed in *E. coli* strain BL21(DE3) as an *N*-terminal His_6-tag fusion and purified by sequential metal affinity, heparin agarose, and gel filtration chromatography, as described previously (28). The FAAH protein contains an *N*-terminal truncation of amino acid residues 1–29, which constitute a predicted transmembrane domain. This deletion has been shown to have no effect on catalytic activity or membrane binding, but enhances expression and purification (28). Enzyme concentrations were calculated assuming an absorbance at 280 nm of 0.8 AU for a 1 mg/ml solution of FAAH (28). Purified protein was stored at –80°C in 10% glycerol until it was used in in vitro assays.

LC-MS analysis. LC-MS analysis was performed using an Agilent 1100 LC/MSD SL instrument (Agilent Technologies), as previously described (54). A Gemini (Phenomenex) C18 reverse-phase column (5 μm, 4.6 × 100 mm) was used together with a precolumn (C18, 3.5 μm, 2 × 20 mm). Mobile phase A consisted of 95%/5% water:methanol, and mobile phase B was made up of 60%/35%/5% 2-propanol:methanol:water. Both A and B were supplemented with 0.1% ammonium hydroxide as a solvent modifier. The gradient started at 40% B and then linearly increased to 100% B over 10 minutes. MS analysis was performed with an electrospray source ionization (ESI) interface. The capillary voltage was set to 3.0 kV and the fragmentor voltage to 100 V. The drying gas temperature was 350°C, the drying gas flow was 10 L/min, and the nebulizer pressure was 35 psi.

In vitro FAAH inhibition assays. Inhibitor analysis was carried out in vitro by measuring purified recombinant FAAH activity in the presence of increasing concentrations of inhibitor by following the conversion of anandamide to arachidonic acid. Reactions were conducted in a buffer of 125 mM Tris, 1 mM EDTA, 0.1% Triton X-100, pH 9.0. Purified FAAH (2 nM) was pre-incubated with αGalCer (2 μL, 50× stock in DMSO added to provide 0–20 μM αGalCer) for 10 minutes. Anandamide (2 μL, 50× stock in DMSO) was then added to provide 12.5–100 μM final substrate concentrations. Reactions were subsequently quenched with 0.5 N HCl at 4 time points. Arachidonic acid production was measured by LC-MS (analysis conditions described above) using the peak area under the extracted ion chromatogram and quantified by comparison with a standard product curve (0–250 pmol arachidonic acid) as previously described (54). For all reactions, time courses were chosen such that product formation did not exceed 20%. Over this time range, FAAH showed linear reaction kinetics. Apparent K_m values were calculated from Lineweaver-Burk plots of 4 substrate concentrations run in triplicate, and the inhibitor binding constant, K_i, was calculated from a plot of apparent K_m versus inhibitor concentration.

Bacterial challenge infection. Groups of immunized and naive control mice were challenged i.v. with 1×10^5 CFU *L. monocytogenes*–expressing chicken ovalbumin (43), and spleens and livers were harvested 3 days later. Organs were homogenized in sterile distilled H_2O containing 0.2% NP-40. Tenfold serial dilutions of tissue homogenate were plated on brain-heart infusion agar plates and grown at 37°C for 24 hours before bacterial colonies were counted.

Statistics. Statistical significance was determined using the unpaired, 2-tailed *t* test (Prism; GraphPad Software Inc.). As normality of the data within the overall population could not be unequivocally assumed at given sample sizes, the data were normalized by logarithmic transformation before statistical analysis was performed. In all experiments, differences were considered significant when *P* was less than 0.05.

Immunoprecipitation of FAAH. FAAH was immunoprecipitated from 1.5×10^8 RBL cells and their supernatant (3-day culture in 2% serum) using anti-FAAH monoclonal antibodies immobilized on Affigel-10 beads. After overnight incubation and washes, the acid elution was analyzed by SDS-PAGE and Western blot using polyclonal rabbit anti-FAAH serum. The same procedure was applied to 6 ml of fresh serum from WT or *Faah* KO mice. For detection of direct binding of αGalCer to cellular FAAH, biotinylated αGalCer was mixed with cellular extracts of WT or *Faah* KO liver (0.5% Brij96) and incubated overnight at 4°C with rotation. Capture with streptavidin-sepharose beads was then carried out for 30 minutes. After extensive washing with extraction buffer, the eluted material was run on a 10%–15% SDS-PAGE gel and immunoblotted. Western blot was carried our with polyclonal rabbit anti-FAAH serum. The presence of FAAH in the immunoprecipitation was confirmed by mass spectrometry.

Analysis of lipid transfer activity. Loading of αGalCer into CD1d was determined by stimulation of DN32.D3 hybridoma cells. Empty, plate-bound CD1d (coated overnight at 1 μg/well) was pulsed with αGalCer in the absence or presence of 10 μM FAAH or 10 μM saposin B for 4 hours. After 3 washes, 5×10^4 DN32.D3 hybridoma cells were added per well, and supernatant was collected 24 hours later for analysis of IL-2 concentration. Unloading of CD1d-bound ganglioside GT1b was monitored using isoelectric focusing (IEF) gel electrophoresis. CD1d-GT1b complexes were purified to homogeneity by anion exchange, incubated in 50 mM malonate buffer (pH 5.0) at equimolar ratio (10 μM) with FAAH, with saposin B or in buffer alone for 1 hour at 37°C, and then analyzed by native IEF. The migration of the CD1d band towards the cathode (empty CD1d band at neutral pH) indicates unloading of bound GT1b (net negative charge) from CD1d (55).

Acknowledgments

We would like to thank the personnel of the TSRI mass spectrometry and flow cytometry facilities. This work was supported by NIH grants AI053725 (to P.B. Savage, A. Bendelac, and L. Teyton), AI070390 (to L. Teyton), and DA017259 (to B.F. Cravatt), and by a fellowship from the Swiss National Science Foundation SNF/SSMBS (to S. Freigang).

Received for publication July 8, 2009, and accepted in revised form March 31, 2010.

Address correspondence to: Luc Teyton, Department of Immunology, The Scripps Research Institute, IMM23, room 301, 10550 North Torrey Pines Road, La Jolla, California 92037, USA. Phone: 858.784.2728; Fax: 858.784.8166; E-mail: lteyton@scripps.edu.

1. Brigl M, Brenner MB. CD1: antigen presentation and T cell function. *Annu Rev Immunol*. 2004; 22:817–890.
2. Kronenberg M. Toward an understanding of NKT cell biology: progress and paradoxes. *Annu Rev Immunol*. 2005;23:877–900.
3. Bendelac A, Savage PB, Teyton L. The biology of NKT cells. *Annu Rev Immunol*. 2007;25:297–336.
4. Zhou D, et al. Editing of CD1d-bound lipid antigens by endosomal lipid transfer proteins. *Science*. 2004;303(5657):523–527.
5. Fischer K, et al. Mycobacterial phosphatidylinositol mannoside is a natural antigen for CD1d-restricted T cells. *Proc Natl Acad Sci U S A*. 2004; 101(29):10685–10690.
6. Kinjo Y, et al. Recognition of bacterial glycosphingolipids by natural killer T cells. *Nature*. 2005; 434(7032):520–525.
7. Mattner J, et al. Exogenous and endogenous glycolipid antigens activate NKT cells during microbial infections. *Nature*. 2005;434(7032):525–529.
8. Kinjo Y, et al. Natural killer T cells recognize diacylglycerol antigens from pathogenic bacteria. *Nat Immunol*. 2006;7(9):978–986.
9. Fujii S, Liu K, Smith C, Bonito AJ, Steinman RM. The linkage of innate to adaptive immunity via maturing dendritic cells in vivo requires CD40 ligation in addition to antigen presentation and CD80/86 costimulation. *J Exp Med*. 2004;199(12):1607–1618.
10. Fujii S, Shimizu K, Hemmi H, Steinman RM. Innate Valpha14(+) natural killer T cells mature dendritic cells, leading to strong adaptive immunity. *Immunol Rev*. 2007;220:183–198.
11. Fujii S, Shimizu K, Smith C, Bonifaz L, Steinman RM. Activation of natural killer T cells by alpha-galactosylceramide rapidly induces the full maturation of dendritic cells in vivo and thereby acts as an adjuvant for combined CD4 and CD8 T cell

immunity to a coadministered protein. *J Exp Med*. 2003;198(2):267–279.
12. Hermans IF, et al. NKT cells enhance CD4+ and CD8+ T cell responses to soluble antigen in vivo through direct interaction with dendritic cells. *J Immunol*. 2003;171(10):5140–5147.
13. Galli G, et al. Invariant NKT cells sustain specific B cell responses and memory. *Proc Natl Acad Sci U S A*. 2007;104(10):3984–3989.
14. Cui J, et al. Requirement for Valpha14 NKT cells in IL-12-mediated rejection of tumors. *Science*. 1997;278(5343):1623–1626.
15. Smyth MJ, et al. Differential tumor surveillance by natural killer (NK) and NKT cells. *J Exp Med*. 2000;191(4):661–668.
16. Giaccone G, et al. A phase I study of the natural killer T-cell ligand alpha-galactosylceramide (KRN7000) in patients with solid tumors. *Clin Cancer Res*. 2002;8(12):3702–3709.
17. Nieda M, et al. Therapeutic activation of Valpha24+Vbeta11+ NKT cells in human subjects results in highly coordinated secondary activation of acquired and innate immunity. *Blood*. 2004; 103(2):383–389.
18. Chang DH, et al. Sustained expansion of NKT cells and antigen-specific T cells after injection of alpha-galactosyl-ceramide loaded mature dendritic cells in cancer patients. *J Exp Med*. 2005;201(9):1503–1517.
19. Ishikawa A, et al. A phase I study of alpha-galactosylceramide (KRN7000)-pulsed dendritic cells in patients with advanced and recurrent non-small cell lung cancer. *Clin Cancer Res*. 2005; 11(5):1910–1917.
20. Terabe M, et al. NKT cell-mediated repression of tumor immunosurveillance by IL-13 and the IL-4R-STAT6 pathway. *Nat Immunol*. 2000;1(6):515–520.
21. Hayakawa Y, Takeda K, Yagita H, Van Kaer L, Saiki I, Okumura K. Differential regulation of Th1 and Th2 functions of NKT cells by CD28 and CD40 costimulatory pathways. *J Immunol*. 2001;166(10):6012–6018.
22. Miyamoto K, Miyake S, Yamamura T. A synthetic glycolipid prevents autoimmune encephalomyelitis by inducing TH2 bias of natural killer T cells. *Nature*. 2001;413(6855):531–534.
23. Gumperz JE, Miyake S, Yamamura T, Brenner MB. Functionally distinct subsets of CD1d-restricted natural killer T cells revealed by CD1d tetramer staining. *J Exp Med*. 2002;195(5):625–636.
24. Crowe NY, et al. Differential antitumor immunity mediated by NKT cell subsets in vivo. *J Exp Med*. 2005;202(9):1279–1288.
25. van den Elzen P, et al. Apolipoprotein-mediated pathways of lipid antigen presentation. *Nature*. 2005;437(7060):906–910.
26. Cravatt BF, Giang DK, Mayfield SP, Boger DL, Lerner RA, Gilula NB. Molecular characterization of an enzyme that degrades neuromodulatory fatty-acid amides. *Nature*. 1996;384(6604):83–87.
27. McKinney MK, Cravatt BF. Structure and function of fatty acid amide hydrolase. *Annu Rev Biochem*. 2005;74:411–432.
28. Patricelli MP, Lashuel HA, Giang DK, Kelly JW, Cravatt BF. Comparative characterization of a wild type and transmembrane domain-deleted fatty acid amide hydrolase: identification of the transmembrane domain as a site for oligomerization. *Biochemistry*. 1998;37(43):15177–15187.
29. Bracey MH, Hanson MA, Masuda KR, Stevens RC, Cravatt BF. Structural adaptations in a membrane enzyme that terminates endocannabinoid signaling. *Science*. 2002;298(5599):1793–1796.
30. Cravatt BF, et al. Supersensitivity to anandamide and enhanced endogenous cannabinoid signaling in mice lacking fatty acid amide hydrolase. *Proc Natl Acad Sci U S A*. 2001;98(16):9371–9376.
31. Massa F, et al. The endogenous cannabinoid system protects against colonic inflammation. *J Clin Invest*. 2004;113(8):1202–1209.
32. Karsak M, et al. Attenuation of allergic contact dermatitis through the endocannabinoid system. *Science*. 2007;316(5830):1494–1497.
33. Lichtman AH, Shelton CC, Advani T, Cravatt BF. Mice lacking fatty acid amide hydrolase exhibit a cannabinoid receptor-mediated phenotypic hypoalgesia. *Pain*. 2004;109(3):319–327.
34. Cravatt BF, Saghatelian A, Hawkins EG, Clement AB, Bracey MH, Lichtman AH. Functional disassociation of the central and peripheral fatty acid amide signaling systems. *Proc Natl Acad Sci U S A*. 2004;101(29):10821–10826.
35. Kawano T, et al. CD1d-restricted and TCR-mediated activation of valpha14 NKT cells by glycosylceramides. *Science*. 1997;278(5343):1626–1629.
36. Edwards JL, Apicella MA. The role of lipooligosaccharide in Neisseria gonorrhoeae pathogenesis of cervical epithelia: lipid A serves as a C3 acceptor molecule. *Cell Microbiol*. 2002;4(9):585–598.
37. Alexander JP, Cravatt BF. Mechanism of carbamate inactivation of FAAH: implications for the design of covalent inhibitors and in vivo functional probes for enzymes. *Chem Biol*. 2005; 12(11):1179–1187.
38. Felder CC, et al. Comparison of the pharmacology and signal transduction of the human cannabinoid CB1 and CB2 receptors. *Mol Pharmacol*. 1995;48(3):443–450.
39. Wacnik PW, Luhr KM, Hill RH, Ljunggren HG, Kristensson K, Svensson M. Cannabinoids affect dendritic cell (DC) potassium channel function and modulate DC T cell stimulatory capacity. *J Immunol*. 2008;181(5):3057–3066.
40. Prigozy TI, et al. Glycolipid antigen processing for presentation by CD1d molecules. *Science*. 2001;291(5504):664–667.
41. Liu Y, et al. A modified alpha-galactosyl ceramide for staining and stimulating natural killer T cells. *J Immunol Methods*. 2006;312(1–2):34–39.
42. Zajonc DM, et al. Structure and function of a potent agonist for the semi-invariant natural killer T cell receptor. *Nat Immunol*. 2005;6(8):810–818.
43. Pope C, et al. Organ-specific regulation of the CD8 T cell response to Listeria monocytogenes infection. *J Immunol*. 2001;166(5):3402–3409.
44. Jack RS, et al. Lipopolysaccharide-binding protein is required to combat a murine gram-negative bacterial infection. *Nature*. 1997;389(6652):742–745.
45. Wurfel MM, Kunitake ST, Lichenstein H, Kane JP, Wright SD. Lipopolysaccharide (LPS)-binding protein is carried on lipoproteins and acts as a cofactor in the neutralization of LPS. *J Exp Med*. 1994;180(3):1025–1035.
46. Anderson NL, et al. The human plasma proteome: a nonredundant list developed by combination of four separate sources. *Mol Cell Proteomics*. 2004;3(4):311–326.
47. Hood BL, et al. Investigation of the mouse serum proteome. *J Proteome Res*. 2005;4(5):1561–1568.
48. Karava V, Fasia L, Siafaka-Kapadai A. Anandamide amidohydrolase activity, released in the medium by Tetrahymena pyriformis. Identification and partial characterization. *FEBS Lett*. 2001;508(3):327–331.
49. Karava V, et al. Anandamide metabolism by Tetrahymena pyriformis in vitro. Characterization and identification of a 66 kDa fatty acid amidohydrolase. *Biochimie*. 2005;87(11):967–974.
50. Smyth MJ, et al. Sequential production of interferon-gamma by NK1.1(+) T cells and natural killer cells is essential for the antimetastatic effect of alpha-galactosylceramide. *Blood*. 2002; 99(4):1259–1266.
51. Sasakawa A, et al. Activated liver dendritic cells generate strong acquired immunity in alpha-galactosylceramide treatment. *J Hepatol*. 2009; 50(6):1155–1162.
52. Park SH, Roark JH, Bendelac A. Tissue-specific recognition of mouse CD1 molecules. *J Immunol*. 1998;160(7):3128–3134.
53. Inaba K, et al. Generation of large numbers of dendritic cells from mouse bone marrow cultures supplemented with granulocyte/macrophage colony-stimulating factor. *J Exp Med*. 1992; 176(6):1693–1702.
54. Saghatelian A, McKinney MK, Bandell M, Patapoutian A, Cravatt BF. A FAAH-regulated class of N-acyl taurines that activates TRP ion channels. *Biochemistry*. 2006;45(30):9007–9015.
55. Cantu C 3rd, Benlagha K, Savage PB, Bendelac A, Teyton L. The paradox of immune molecular recognition of alpha-galactosylceramide: low affinity, low specificity for CD1d, high affinity for alpha beta TCRs. *J Immunol*. 2003;170(9):4673–4682.